

RSC Advances



This is an *Accepted Manuscript*, which has been through the Royal Society of Chemistry peer review process and has been accepted for publication.

Accepted Manuscripts are published online shortly after acceptance, before technical editing, formatting and proof reading. Using this free service, authors can make their results available to the community, in citable form, before we publish the edited article. This *Accepted Manuscript* will be replaced by the edited, formatted and paginated article as soon as this is available.

You can find more information about *Accepted Manuscripts* in the [Information for Authors](#).

Please note that technical editing may introduce minor changes to the text and/or graphics, which may alter content. The journal's standard [Terms & Conditions](#) and the [Ethical guidelines](#) still apply. In no event shall the Royal Society of Chemistry be held responsible for any errors or omissions in this *Accepted Manuscript* or any consequences arising from the use of any information it contains.

ARTICLE

A study of the growth-time effect on graphene layer number based on Cu–Ni bilayer catalyst system

Cite this: DOI: 10.1039/x0xx00000x

Tao Wu^{a,b}, Zhiduo Liu^b, Guoxin Chen^b, Dan Dai^b, Hongyan Sun^b, Wen Dai^b, Nan Jiang^{b,*}, Ye Hua Jiang^{a,*}, Cheng-Te Lin^{b,*}Received oothxxxx 201x
Accepted oothxxxx 201x

DOI: 10.1039/x0xx00000x

www.rsc.org/

The evolution of graphene-based electronic, optoelectronic, and sensing devices is growing at a fast pace in the recent decade, due to the rapid development of the manufacturing technology for high-quality graphene. However, the absence of controllability of graphene thickness sets an additional barrier for device applications. Here, we demonstrate that the number of graphene layers can be well controlled by adjusting the Cu–Ni catalyst composition and the reaction time. The Cu–Ni bilayer catalysts are prepared by sputtering Ni and then Cu films on SiO₂/Si substrate with various film thicknesses. With the increase of the growth time, single-layer graphene would be formed on the Cu-rich catalysts, whereas bilayer to few-layer graphene can be obtained on the Ni-rich films. In addition, the formation of single-layer to bilayer graphene as a function of time is attributed to the synergic effect of Cu and Ni catalysts with 1:1 composition. The precise control of graphene layer number enables the further development of the advanced electronics and sensors.

1. Introduction

Graphene has attracted great attention of both the scientific community and the industry in the recent decade, due to its fascinating properties and wide potential applications.¹ In the definition, graphene is a one-atom-thick carbon layer composed of sp²-bonded carbon atoms and packed into a honeycomb lattice.² Before graphene was successfully isolated from graphite in 2004,³ according to Mermin–Wagner theorem, a single-atom-thick material was considered unable to exist at room temperature in a thermodynamic stable state.⁴ The discovery of graphene substantially broadens the researchers' perspective of nanoscience and nanotechnology, leading to the following findings of other 2D atomic materials.⁵ Nowadays, hundreds-meter-long graphene films can be prepared by "bottom-up" growth technique (chemical vapor deposition, CVD),⁶ and single- to multi-layer graphene sheets with production capacity of tons can be made by "top-down" process (intercalation/exfoliation of graphite).⁷ Depending on the manufacturing methods, graphene and its derivatives exhibit versatile properties to accommodate a broad range of applications in aerospace, biotechnology, energy, thermal management etc.^{8–10}

Among them, the development of advanced electronic/optoelectronic devices and sensors is particularly promising, due to graphene's ultrafast electron mobility,¹ robust flexibility,^{11, 12} transparency in visible light region,¹³ and good mechanical strength.¹⁴ Therefore, the pursuit of high-quality graphene with controllable layer number and properties is needed and challenging.

CVD technique has been widely employed to prepare large-area, low-defect graphene films, because of the advantages of low-cost, ease of scale-up, and technical simplicity.¹⁵ A CVD process for graphene growth involve the decomposition of carbon feedstock (either gaseous or solid hydrocarbons) at high temperature with the aid of the catalysts, such as Cu,^{16–18} Ni,^{19–22} Pt,^{23, 24} Ga,²⁵ NiAl₂O₄²⁶ etc. Although great efforts have been done to grow graphene on polycrystalline Ni or Cu foils,^{17, 27, 28} however, the lack of controllability of graphene layer number creates additional barriers for application in electronics.²⁹ Graphene films on polycrystalline Ni are usually grown as few layers, which can be attributed to the non-equilibrium precipitation of carbon atoms from Ni during the cooling step.²⁷ Single-layer graphene is preferred to form on the Cu surface based on the effect of kinetically self-limiting deposition.³⁰ In recent years, the preparation of graphene by CVD using Cu/Ni alloy catalyst grows up rapidly, in order to precisely control the layer number, uniformity, and the geometry of graphene.^{31–36} Wan et al. reported the "smart Janus" substrate made of Cu/Ni alloy on Cu foil to grow graphene with defined thickness, at a wide temperature window.³² Wu et al. obtained a 1.5-inch-large, single-crystal graphene monolayer by local feeding CH₄ to a target substrate with Cu₈₅Ni₁₅ alloy catalyst.³³ However, in the cases mentioned above, it is still not clear what the role of the reaction time and the Cu–Ni ratio played during the CVD process, and how both parameters work on the result of graphene layer number.

¹ Faculty of Materials Science and Engineering, Kunming University of Science and Technology, Kunming 650093, China

² Key Laboratory of Marine Materials and Related Technologies, Zhejiang Key Laboratory of Marine Materials and Protective Technologies, Ningbo Institute of Materials Technology and Engineering (NIMTE), Chinese Academy of Sciences, Ningbo 315201, China. Email address: jiangnan@nimte.ac.cn; jiangyehua@kmust.deu.cn; linzhengde@nimte.ac.cn

In this study, we investigated the number of graphene layers obtained on Cu–Ni thin films with various alloy compositions by thermal CVD. Instead of a fixed Cu–Ni ratio, Cu–Ni bilayer catalysts with different thickness ratios were deposited on the substrate for graphene growth. Based on this sandwiched structure (Cu/Ni/SiO₂/Si), the composition of the catalyst would dynamically vary during the CVD process, because of the interdiffusion of Cu/Ni layers and Cu evaporation at high temperature. The graphene layer number and the surface morphology of Cu–Ni bilayer catalyst, as a function of the reaction time, will be examined and discussed.

2. Experimental

For preparation of the catalyst layers, Ni film was firstly deposited on 300 nm-thick SiO₂/Si substrates using mini-type ion sputtering apparatus (Quorum 150T ES, UK), and then Cu layer was covered on the Ni surface by thermal evaporation (Beijing Tainuo Co., ZHD-300M2, China). The desorption rate of both Cu and Ni layers was evaluated separately to keep the total thickness of Cu–Ni bilayer constant (450 nm) in all samples. Three different ratios in thickness (3:1, 1:1, 1:3) for Cu–Ni films were prepared, e.g.: 3:1 means the film consists of Cu and Ni (337.5 + 112.5 nm) in thickness. A thermal CVD system (BTF-1200C-II-SL, Anhui BEQ Equipment Tech. China) was employed to grow graphene. The substrates (Cu/Ni/SiO₂/Si) were loaded into the tube furnace, followed by heating to 750 °C at a rate of 10 °C/min. The samples were annealed at 750 °C for 25 min with the flow of H₂/Ar (215/400 sccm, pressure: 250 Torr), and then rapidly heated to 900 °C. When 900 °C was reached, a gas mixture of CH₄/H₂ (75/15 sccm, pressure: 1.5 Torr) was introduced for graphene growth. After 5 – 15 min reaction, the furnace was cooled down to room temperature at a cooling rate of 20 °C/min. The details can be found elsewhere³⁷. The obtained samples were characterized by Raman spectroscopy (Renishaw plc, Wotton-under-Edge) employing a laser wavelength of 532 nm, field emission scanning electron microscopy (FE-SEM, QUANTA FEG250). The composition of Cu–Ni bilayer after CVD growth was determined by energy dispersive spectrometer (EDS, Oxford X-Max^N).

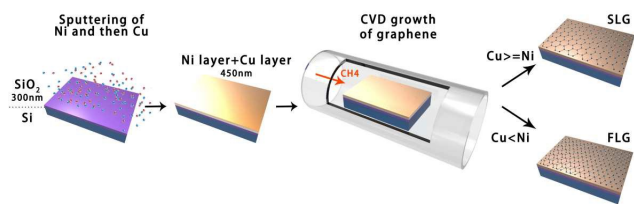


Figure 1. A schematic illustration of the formation of graphene on Cu–Ni bilayer catalysts by thermal CVD.

3. Results and discussion

Figure 1 shows our concept of graphene growth process on Cu–Ni bilayer catalyst system by thermal CVD. Ni film was first deposited on SiO₂ (300 nm)/Si substrate, followed by coating with Cu layer, resulting in the formation of a

sandwiched structure of Cu/Ni/SiO₂/Si with a fixed total thickness (450 nm) of Cu–Ni bilayer. The samples were annealed at 750 °C for reduction of native oxides on the surface of the metal catalyst, and then heated up to 900 °C to grow graphene with different reaction time. In the common CVD process, the reaction temperature of graphene on Cu ranges from 950 – 1,000 °C,³⁸ and the cases on Ni can be lower (> 850 °C).³⁹ This can be attributed to the very low solubility between carbon and copper, leading to higher decomposition energy of CH₄ with the assistance of Cu catalyst. The incorporation of Ni into Cu as a binary catalyst results in a good balance between lower growth temperature (\approx 900 °C) and the graphene quality. Moreover, the poor wettability of Cu on SiO₂/Si may lead to the fast evaporation of Cu film during the CVD process. Therefore, the insertion of a Ni layer at the interface of Cu and the substrate is beneficial to the thermal stability of the catalyst system.

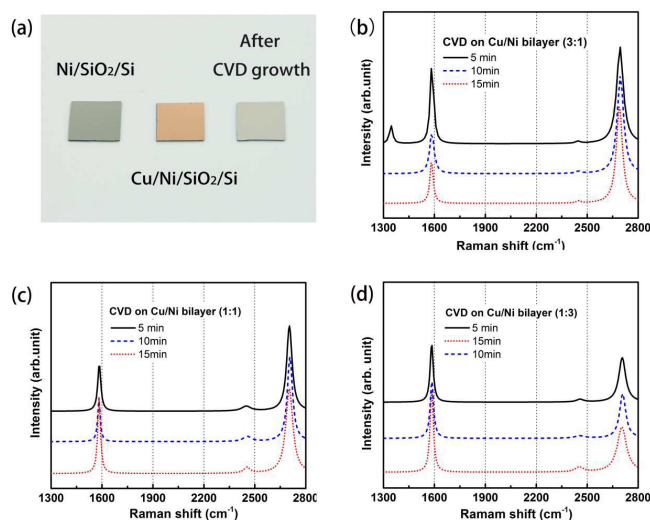


Figure 2. (a) A photograph of the samples after catalyst deposition and CVD growth. The typical Raman spectra of graphene grown on the catalysts composed of; (b) 3:1; (c) 1:1; (d) 1:3 Cu–Ni bilayer and different growth time.

A photograph of the samples after Ni, Cu–Ni bilayer deposition and graphene growth, respectively, is presented in **Figure 2(a)**. It can be seen that the color of the samples changes from gray (Ni), bronze (Cu–Ni), to light gray (Cu/Ni alloy) after CVD. Raman spectra taken from the graphene films grown with various Cu–Ni compositions and reaction time are shown in **Figure 2(b–d)**. Note that all the spectra were reconstructed using Gaussian fit to evaluate the peak height and full width at half maximum (FWHM). The examples of the original and Gaussian fitted plots are shown in **Figure S1**. In **Figure 2(b)**, the Cu/Ni ratio of 3:1 means that the catalyst film is composed of 337.5 nm-thick Cu and 112.5 nm-thick Ni. Due to the similar density (Cu: 8.92, Ni: 8.90 g/cm³), the thickness ratio of Cu–Ni can be considered as same as the ratio of the weight percent, e.g.: 3:1 = 75 wt% Cu. The spectra in **Figure 2(b–d)** exhibit the typical peaks of graphene: G-band at 1579 – 1588 cm⁻¹ is caused by the stretching-vibration mode of sp² sites, such as C=C bonds in aromatic compounds,⁴⁰ while 2D-band located at 2688 – 2699 cm⁻¹

is formed of a double-resonance process.^{41–43} The degree of sp^2 -hybridized C–C bonding in graphene can be described by I_{2D}/I_G ratio, which is commonly used to estimate the graphene layer number combining the consideration of 2D-band FWHM.^{44,45} A tiny peak called D-band appears at 1350 cm^{-1} in **Figure 2(b)** for the sample after 5-min growth. The D-band is attributed to the bond-angle disorder induced by the formation of sp^3 bonds, which indicates the degree of the defects in graphene structure.⁴⁰ The absence of the D-band in **Figure 2** suggests the formation of high-quality graphene films using Cu–Ni bilayer catalyst system.

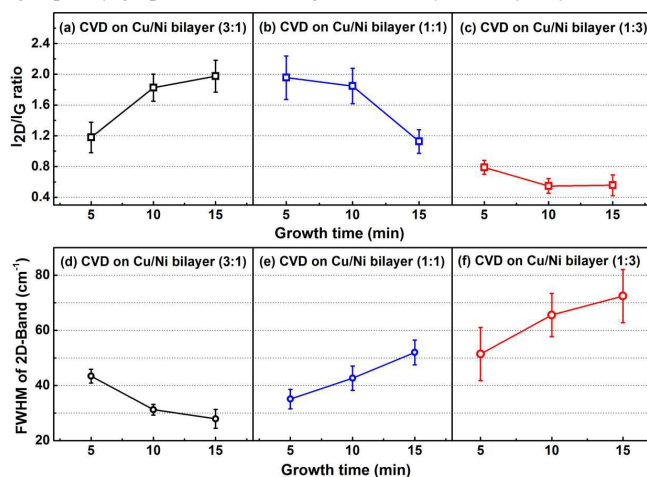


Figure 3. The calculated I_{2D}/I_G ratios and 2D-band FWHM of graphene films grown on the bilayer catalysts with Cu–Ni composition of: (a) (d) 3:1; (b) (e) 1:1; and (c) (f) 1:3, respectively.

The variations of I_{2D}/I_G ratios and the FWHM of the 2D-band calculated from **Figure 2(b–d)** are summarized in **Figure 3**. Interestingly, we noticed that the I_{2D}/I_G ratios and 2D-band FWHM show a regular change between the samples, even though which were prepared with different Cu–Ni compositions and growth time. In the case of Cu-rich catalyst (Cu/Ni = 3:1, **Figure 3(a)**), the I_{2D}/I_G ratio of the samples increases from 1.18 to 1.97 as the growth time increases from 5 to 15 min. The disappearance of D-band (**Figure 2(b)**), and the rise of I_{2D}/I_G ratio indicate that a continuous single-layer graphene is gradually formed from nanocrystalline domains.⁴⁶ The narrow 2D-band for the FWHM ranging from 27.9 to 43.4 in **Figure 3(d)** confirms the single-layer nature of graphene.²⁷ In contrast, when the time increases, the I_{2D}/I_G ratio decreases from 1.96 to 1.13 with the increase of FWHM from 35.1 to 52.0, for the samples obtained on Cu–Ni catalyst with 1:1 composition, as exhibited in **Figure 3(b) and (e)**, respectively. In the condition of Cu/Ni = 1:1, we found that the resulting number of graphene layers shows a significant dependence on the reaction time. Single-layer graphene could be deposited at the initial stage (5 min), and then bilayer graphene film would be formed for longer growth time (15 min).^{47,48} In Ni-rich catalyst system (Cu/Ni = 1:3, **Figure 3(c)**), the graphene layer number starts as bilayer, and then goes to few-layer with the increase of the reaction time. The symmetrical 2D-band (**Figure 2(d)**) indicates that the thickness of the sample after 15-min growth does not exceed 5 layers of graphene.⁴⁴ Briefly, we conclude that single-, bilayer, and few-layer graphene films can

be prepared separately by adjusting Cu–Ni bilayer composition and the growth time.

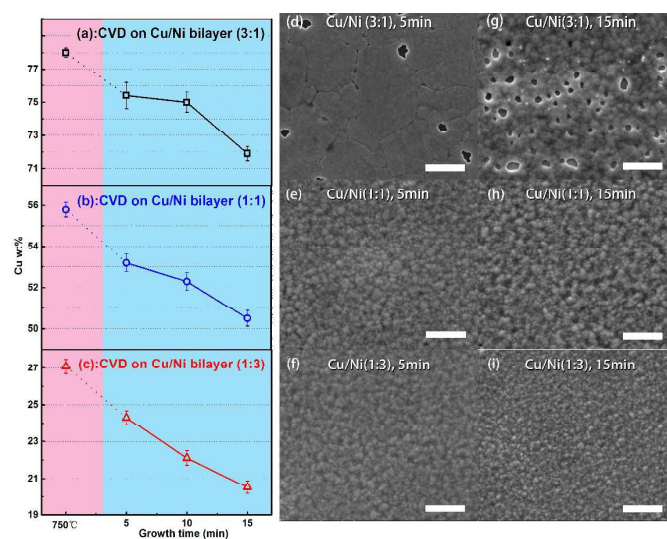


Figure 4. (a)–(c) The variation of Cu wt% in different bilayer catalysts during CVD process. The surface SEM images of the samples prepared at 900 °C for (d)–(f) 5-min and (g)–(i) 15-min reaction with different catalyst compositions. The scale bar in the SEM images is 10 μm .

To interpret the formation mechanism of different numbers of graphene layers with bilayer catalysts, the Cu–Ni compositions during the CVD process have been determined by EDS, as shown in **Figure 4(a)–(c)**. Although Cu and Ni thin films were deposited individually, the solid solution phase of Cu–Ni was formed at 750 – 900 °C. In the Cu-rich case (Cu/Ni = 3:1, **Figure 4(a)**), the surface of catalyst films contains 71.9 and 75.4 wt% of Cu after reaction for 5 and 15 min at 900 °C, respectively. It is demonstrated that the growth of single-layer graphene follows the self-limiting mechanism when Cu is dominant in the catalyst system, whereas the segregation mechanism works to grow few-layer graphene under the condition of Ni-rich catalyst (Cu: 20.5 – 24.3 wt%, **Figure 4(c)**). The decrease of Cu wt% as a function of time in **Figure 4(a)–(c)** is due to the partial evaporation of Cu at high temperature (900 °C) and low pressure (1.5 Torr), based on the difference of the melting point between Cu (1,085 °C) and Ni (1,455 °C). We noticed that the surface morphology of Cu–Ni bilayer after CVD growth, as well as the quality of graphene, would be affected by the Cu evaporation, as seen in the SEM images of **Figure 4(d)–(i)** and **Figure S2**. For comparison, **Figure S3** presents the SEM images of the catalyst films treated under the same CVD conditions without the introduction of CH_4 . We noticed that the formation of graphene enables to suppress the Cu evaporation and the boundary of the graphene domains can be clearly seen after the CVD growth (**Figure S4**). In **Figure 4(d) and (g)**, the Cu-rich catalyst layer becomes more porous as the reaction time increases, which makes the graphene film incomplete. The evaporation and dewetting behavior of Cu on SiO_2/Si were even stronger when only Cu was deposited as the catalyst, leading to the degradation of graphene quality, as shown in **Figure S5**. It is of more interest to investigate

the growth mechanism of single- to bilayer graphene on Cu–Ni catalyst with 1:1 composition (**Figure 4(b)**). Because Cu content does not change a lot (50.5 – 53.2 wt%) during 5 – 15 min reaction, the increase of graphene layer number should mainly depend on the growth time. This can be attributed to the synergic effect of the combination of a carbon-rejecting component (Cu) and a carbon-dissolving component (Ni), which enables to regulate the C content at the catalyst surface. As the time increases, more but limiting concentration of C atoms would be dissolved in dilute Ni and then released to the surface in the cooling step, resulting in the formation of bilayer graphene. The same results can be observed in the TEM images (**Figure S6**), confirming the above conclusion.

4. Conclusions

In summary, we demonstrate that the number of graphene layers grown on Cu–Ni bilayer catalysts can be well controlled, by adjusting the Cu–Ni composition and the growth time. Although the concept of control of graphene layer thickness using $\text{Cu}_x\text{Ni}_{1-x}$ catalyst has been proved by Choi et al.,³¹ we verify that the reaction time is also a key factor to influence the resulting number of graphene layers, as well as the quality of graphene. As time increases, graphene grown on Cu-rich catalyst surface (Cu/Ni = 3:1) remains single-layer, whereas bilayer and then few-layer graphene can be obtained using Ni-rich catalysts (Cu/Ni = 1:3). Moreover, in the case of Cu–Ni catalysts with 1:1 composition, the formation of single-layer to bilayer graphene as a function of time is attributed to the synergic effect of Cu for C-rejection and Ni for C-dissolution, which enable the growth of bilayer graphene based on the regulation of C concentration at the Cu–Ni surface.

Acknowledgements

We acknowledge the financial support from Chinese Academy of Science for Hundred Talents Program, Chinese Central Government for Thousand Young Talents Program, and The Key Technology of Nuclear Energy (2014 CAS Interdisciplinary Innovation Team). This work was also supported by the National Science Foundation of Zhejiang Province (Grant No. Q15E020007) and the Ningbo Natural Science Foundation (Grant No. 2015A610082).

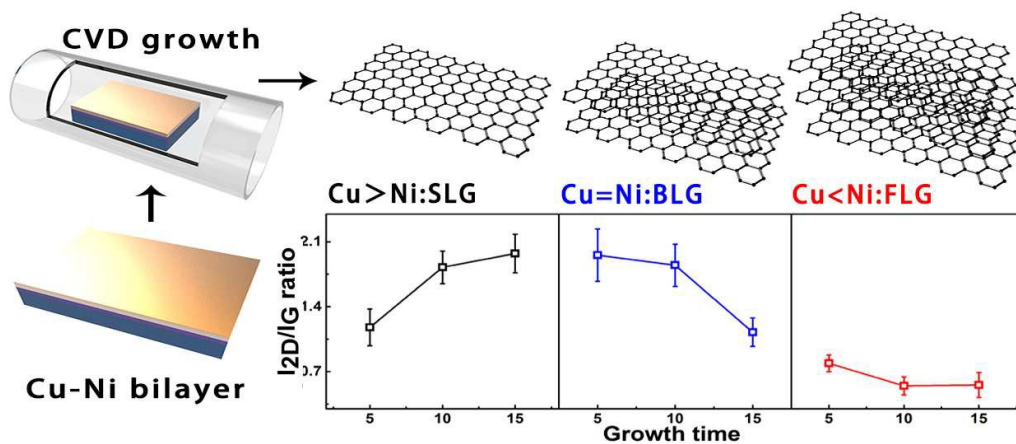
References

1. T. Hesjedal, *Appl. Phys. Lett.*, 2011, **98**, 133106.
2. A. Bianco, H.-M. Cheng, T. Enoki, Y. Gogotsi, R. H. Hurt, N. Koratkar, T. Kyotani, M. Monthieux, C. R. Park, J. M. D. Tascon and J. Zhang, *Carbon*, 2013, **65**, 1-6.
3. K. S. Novoselov, A. K. Geim, S. V. Morozov, D. Jiang, Y. Zhang, S. V. Dubonos, I. V. Grigorieva and A. A. Firsov, *Science*, 2004, **306**, 666-669.
4. N. D. Mermin and H. Wagner, *Phys. Rev. Lett.*, 1966, **17**, 1133-1136.
5. K. Novoselov, D. Jiang, F. Schedin, T. Booth, V. Khotkevich, S. Morozov and A. Geim, *P. Natl. Acad. Sci. USA.*, 2005, **102**, 10451-10453.
6. T. Kobayashi, M. Bando, N. Kimura, K. Shimizu, K. Kadono, N. Umezumi, K. Miyahara, S. Hayazaki, S. Nagai, Y. Mizuguchi, Y. Murakami and D. Hobara, *Appl. Phys. Lett.*, 2013, **102**, 023112.
7. C.-M. Gee, C.-C. Tseng, F.-Y. Wu, H.-P. Chang, L.-J. Li, Y.-P. Hsieh, C.-T. Lin and J.-C. Chen, *Displays*, 2013, **34**, 315-319.
8. C.-H. Chen, C.-T. Lin, W.-L. Hsu, Y.-C. Chang, S.-R. Yeh, L.-J. Li and D.-J. Yao, *Nanomed-Nanotechnol.*, 2013, **9**, 600-604.
9. S. M. Jung, D. L. Mafra, C.-T. Lin, H. Y. Jung and J. Kong, *Nanoscale*, 2015, **7**, 4386-4393.
10. W. Dai, J. Yu, Y. Wang, Y. Song, F. E. Alam, K. Nishimura, C.-T. Lin and N. Jiang, *J. Mater. Chem. A*, 2015, **3**, 4884-4891.
11. Y. Hu and X. Sun, *J. Mater. Chem. A.*, 2014, **2**, 10712-10738.
12. G. Zhou, F. Li and H.-M. Cheng, *Energ. Environ. Sci.*, 2014, **7**, 1307-1338.
13. Q. Li, B. Guo, J. Yu, J. Ran, B. Zhang, H. Yan and J. R. Gong, *J. Am. Chem. Soc.*, 2011, **133**, 10878-10884.
14. C. Lee, X. Wei, J. W. Kysar and J. Hone, *Science*, 2008, **321**, 385-388.
15. G. Jo, M. Choe, C.-Y. Cho, J. H. Kim, W. Park, S. Lee, W.-K. Hong, T.-W. Kim, S.-J. Park and B. H. Hong, *Nanotechnology*, 2010, **21**, 175201.
16. L. Gao, W. Ren, J. Zhao, L.-P. Ma, Z. Chen and H.-M. Cheng, *Appl. Phys. Lett.*, 2010, **97**, 183109.
17. X. Li, W. Cai, J. An, S. Kim, J. Nah, D. Yang, R. Piner, A. Velamakanni, I. Jung and E. Tutuc, *Science*, 2009, **324**, 1312-1314.
18. X. Li, C. W. Magnuson, A. Venugopal, J. An, J. W. Suk, B. Han, M. Borysiak, W. Cai, A. Velamakanni and Y. Zhu, *Nano Lett.*, 2010, **10**, 4328-4334.
19. R. Addou, A. Dahal, P. Sutter and M. Batzill, *Appl. Phys. Lett.*, 2012, **100**, 021601.
20. Q. Yu, J. Lian, S. Siriponglert, H. Li, Y. P. Chen and S.-S. Pei, *Appl. Phys. Lett.*, 2008, **93**, 113103.
21. Y. Zhang, L. Gomez, F. N. Ishikawa, A. Madaria, K. Ryu, C. Wang, A. Badmaev and C. Zhou, *J. Phys. Chem. Lett.*, 2010, **1**, 3101-3107.
22. C. Chen, D. Dai, G. Chen, J. Yu, K. Nishimura, C.-T. Lin, N. Jiang and Z. Zhan, *Appl. Surf. Sci.*, 2015, **346**, 41-45.
23. H. Ueta, M. Saida, C. Nakai, Y. Yamada, M. Sasaki and S. Yamamoto, *Surf. Sci.*, 2004, **560**, 183-190.
24. P. Sutter, J. T. Sadowski and E. Sutter, *Phys. Rev. B.*, 2009, **80**, 245411.
25. L. Tan, M. Zeng, Q. Wu, L. Chen, J. Wang, T. Zhang, J. Eckert, M. H. Rummeli and L. Fu, *Small*, 2015, **11**, 1840-1846.
26. X. Liu, T. Lin, M. Zhou, H. Bi, H. Cui, D. Wan, F. Huang and J. Lin, *Carbon*, 2014, **71**, 20-26.
27. A. Reina, X. Jia, J. Ho, D. Nezich, H. Son, V. Bulovic, M. S. Dresselhaus and J. Kong, *Nano Lett.*, 2008, **9**, 30-35.
28. K. S. Kim, Y. Zhao, H. Jang, S. Y. Lee, J. M. Kim, K. S. Kim, J.-H. Ahn, P. Kim, J.-Y. Choi and B. H. Hong, *Nature*, 2009, **457**, 706-710.
29. N. Liu, L. Fu, B. Dai, K. Yan, X. Liu, R. Zhao, Y. Zhang and Z. Liu, *Nano Lett.*, 2010, **11**, 297-303.
30. R. Kikowatz, K. Flad and G. Hörz, *J. Vac. Sci. Technol. A.*, 1987, **5**, 1009-1014.
31. H. Choi, Y. Lim, M. Park, S. Lee, Y. Kang, M. S. Kim, J. Kim and M. Jeon, *J. Mater. Chem. C*, 2015, **3**, 1463-1467.
32. D. Wan, T. Lin, H. Bi, F. Huang, X. Xie, I. Chen and M. Jiang, *Adv. Funct. Mater.*, 2012, **22**, 1033-1039.
33. T. Wu, X. Zhang, Q. Yuan, J. Xue, G. Lu, Z. Liu, H. Wang, H. Wang, F. Ding and Q. Yu, *Nature Mater.*, 2015.
34. Q. Wang, L. Wei, M. Sullivan, S.-W. Yang and Y. Chen, *RSC Adv.*, 2013, **3**, 3046-3053.

35. E. Kim, Y. S. Kim, J. Park, S. Hussain, S.-H. Chun, S. J. Kim, K.-S. An, W.-J. Lee, W.-G. Lee and J. Jung, *RSC Adv.*, 2014, **4**, 63349-63353.
36. B. M. Kellie, A. C. Silleck, K. Bellman, R. Snodgrass and S. Prakash, *RSC Adv.*, 2013, **3**, 7100-7105.
37. C.-Y. Su, A.-Y. Lu, C.-Y. Wu, Y.-T. Li, K.-K. Liu, W. Zhang, S.-Y. Lin, Z.-Y. Juang, Y.-L. Zhong and F.-R. Chen, *Nano Lett.*, 2011, **11**, 3612-3616.
38. A. L. Walter, S. Nie, A. Bostwick, K. S. Kim, L. Moreschini, Y. J. Chang, D. Innocenti, K. Horn, K. F. McCarty and E. Rotenberg, *Phys. Rev. B*, 2011, **84**, 195443.
39. K. Takahashi, K. Yamada, H. Kato, H. Hibino and Y. Homma, *Surf. Sci.*, 2012, **606**, 728-732.
40. D. J. Late, U. Maitra, L. Panchakarla, U. V. Waghmare and C. Rao, *J. Phys- Condens. Matt.*, 2011, **23**, 055303.
41. A. C. Ferrari and J. Robertson, *Phys. Rev. B*, 2000, **61**, 14095.
42. A. Gupta, G. Chen, P. Joshi, S. Tadigadapa and P. Eklund, *Nano Lett.*, 2006, **6**, 2667-2673.
43. A. Ferrari, J. Meyer, V. Scardaci, C. Casiraghi, M. Lazzeri, F. Mauri, S. Piscanec, D. Jiang, K. Novoselov and S. Roth, *Phys. Rev. Lett.*, 2006, **97**, 187401.
44. Z. Ni, H. Wang, J. Kasim, H. Fan, T. Yu, Y. Wu, Y. Feng and Z. Shen, *Nano Lett.*, 2007, **7**, 2758-2763.
45. S. Chen, W. Cai, R. D. Piner, J. W. Suk, Y. Wu, Y. Ren, J. Kang and R. S. Ruoff, *Nano Lett.*, 2011, **11**, 3519-3525.
46. B. Krauss, T. Lohmann, D.-H. Chae, M. Haluska, K. von Klitzing and J. H. Smet, *Phys. Rev. B*, 2009, **79**, 165428.
47. Z. Sun, Z. Yan, J. Yao, E. Beitler, Y. Zhu and J. M. Tour, *Nature*, 2010, **468**, 549-552.
48. Z. Peng, Z. Yan, Z. Sun and J. M. Tour, *ACS Nano*, 2011, **5**, 8241-8247.

Graphical Abstract

Table of contents entry:



Highlight:

Graphene layer number can be controlled by changing Cu–Ni ratio and growth time. Single- and few-layer graphene are formed separately on Cu- and Ni-rich catalysts. The growth of bilayer graphene is attributed to the synergic effect of Cu and Ni (1:1).